ISSN: 1410-8917
Jurnal Kimia Sains & Aplikasi
e-ISSN: 2597-9914

Jurnal Kimia Sains dan Aplikasi 28 (3) (2025): 115-121
Jurnal Kimia Sains dan Aplikasi
Journal of Scientific and Applied Chemistry
Journal homepage: http://ejournal.undip.ac.id/index.php/ksa

Utilization of Shrimp Shell Waste as Nitrogen Source in N-Doped TiO_2 for Degradation of Polyethylene Microplastics

Nurhasni [1], Annisaul Izzah [1], Aisyah Rahma Dwitami [1], Yuza Ahmad Gumilang [1], Zilfa [1], Diana Vanda Wellia [1,*]

[1] Department of Chemistry, Faculty of Mathematics and Natural Sciences, Universitas Andalas, Padang, Indonesia

* Corresponding author: nandadiana@sci.unand.ac.id

https://doi.org/10.14710/jksa.28.3.115-121

Article Info

Article history:

Received: 15th August 2024
Revised: 08th April 2025
Accepted: 08th April 2025
Online: 30th April 2025

Keywords:
N-doped TiO_2; shrimp shells; solvothermal; photocatalytic; microplastics

Abstract

Microplastic pollution presents a significant challenge globally, posing serious threats to aquatic ecosystems. This study explores the photocatalytic degradation of microplastics in aqueous solutions by applying nitrogen-doped TiO_2 (N-TiO_2) nanoparticles under visible light. The N-TiO_2 nanoparticles were synthesized via the solvothermal method, utilizing chitosan derived from shrimp shell waste as a nitrogen source. The photocatalytic efficacy of the N-TiO_2 nanoparticles was assessed for degrading model polyethylene microplastics, illuminated by a 50-watt LED lamp. Characteristic peak shifts in the FTIR absorption spectrum, notably at 3429 cm^{-1} to lower wavenumbers, and diminished amide I absorption at 1621 cm^{-1}, confirmed the successful extraction of chitosan from shrimp shell waste. The synthesized N-TiO_2 nanoparticles were in the pure anatase phase, exhibited a reduced bandgap of 2.97 eV, and showed enhanced absorption in the visible light spectrum (λ = 400 – 800 nm) compared to undoped TiO_2. The incorporation of nitrogen into the TiO_2 matrix was validated by vibration bands at approximately 1035 cm^{-1} and 535 cm^{-1}, corresponding to the Ti—N and Ti—O—Ti bonds, respectively. Optimal results were attained with TiO_2 nanoparticles doped with 50% nitrogen, achieving a degradation rate of approximately 30.45% of a 250 mg/L microplastic solution over 50 hours of visible light exposure—nearly six times more effective than undoped TiO_2. This study highlights the sustainable use of shrimp shell waste as a nitrogen source for enhancing TiO_2 nanoparticles, showcasing their potential for environmental remediation applications.

1. Introduction

Recently, microplastics, defined as small plastic particles less than 5 mm in size, have threatened the survival of organisms on land and in the ocean [1]. The World Health Organization (WHO) states that microplastic pollutants have been detected in seawater, wastewater, air, and drinking water, including bottled and refilled water [2]. Research conducted by scientists at the Department of Chemistry, State University of New York, tested 259 bottles of drinking water from 11 brands sold in 8 countries, and discovered that 93% of these bottles contained microplastics. One sample from Indonesia contained an average of 382 microplastic particles per liter, with sizes ranging from 6.5 to over 100 µm [3]. Microplastics can absorb toxic chemical compounds from the surrounding environment, making them hazardous and carcinogenic pollutants. When these particles accumulate in the human body, they can lead to various health issues, including clots in the digestive tract, blockages in the bloodstream, kidney disorders, and even cancer [4]. The most commonly used type of microplastic is polyethylene. This material is frequently used in packaging, tableware, and garbage bags, and is responsible for 64% of the waste generated from end-of-life synthetic plastics [2].

Several methods for degrading microplastics have been conducted, including ion plasma technology [5], coagulation, biodegradation, and photocatalysis [6]. Among these methods, photocatalysis using semiconducting metal oxides such as TiO_2 is considered a promising method due to its high degradation efficiency, low cost, reliance on abundant sunlight, and generation of harmless by-products [7]. Photocatalytic performance can be enhanced by optimizing the size of TiO_2 particles, particularly by utilizing nanoparticles. Materials on the nanoscale (1-100 nm) exhibit significantly improved properties compared to bulk materials, even with the same crystal structure [2].

The limitation of TiO_2 nanoparticles is that they can only absorb UV light (5% of the sunlight spectrum) due to their wide band gap [3]. Therefore, improving the efficiency of TiO_2 absorption, particularly under visible light, by doping with nitrogen on the surface of the TiO_2 lattice, presents a promising approach. Research by Yu and Lv [8] shows that nitrogen doping can narrow the band gap of TiO_2, enhancing its optical properties. The nanostructure of doped TiO_2 also significantly increases its specific surface area compared to the smooth surface of undoped TiO_2. This structure can facilitate charge transfer and improve photoelectrochemical activity [4].

Nitrogen sources employed in the synthesis of N- doped TiO_2 nanoparticles are generally derived from chemicals, including urea, triethylamine, ammonia, ammonium chloride, hydrazine, thiourea, and ammonium nitrate [5]. Nevertheless, the drawbacks of using these chemicals are high toxicity, high cost, significant energy consumption, and environmental concerns. An eco-friendly nitrogen source for producing N-doped TiO_2 comes from biomass waste [2]. One of the biomass wastes that has the potential to serve as a nitrogen source in the manufacture of N-doped TiO_2 is shrimp shell waste. This is due to the chitin content in shrimp shell waste, which reaches 42-57%, higher than that of squid, which only reaches 40%, and shellfish, which contains 14-35% [6]. However, chitin exhibits limited physical properties, characterized by high hydrophobicity and insolubility in common organic and inorganic solvents, so chitin must be modified into chitosan through a deacetylation process. Chitosan is a chitin derivative that contains abundant polar functional groups such as $—NH_2$ [7]. These functional groups can act as a nitrogen source in the synthesis of N-doped TiO_2 nanoparticles.

In a previous study, Ariza-Tarazona *et al.* [9] investigated the degradation of PET microplastics utilizing a C, N-TiO_2/SiO_2 semiconductor and reported a mass loss ranging from 9.35% to 16.22% [10]. Through comprehensive literature reviews, it has been identified that utilizing shrimp shell waste as a nitrogen source for synthesizing N-doped TiO_2 nanoparticles has not been previously reported. This aspect introduces a novel approach to the development of nanomaterial synthesis. Consequently, this research seeks to synthesize N-doped TiO_2 nanoparticles via the solvothermal method, employing chitosan extracted from shrimp shells as the nitrogen source. The aim is to evaluate the impact of this synthesis method on the nanoparticles' properties and to assess their photocatalytic activity against polyethylene microplastic pollutant models.

2. Experimental

2.1. Materials

The materials used in this research were 1 M titanium tetrachloride ($TiCl_4$, Merck), shrimp shells waste (sample), deionized water, distilled water, ethanol (C_2H_5OH, Merck), sodium hydroxide (NaOH, Merck), hydrochloric acid (HCl, Merck), acetate (CH_3COONa) pH 3, polyethylene (as a model pollutant).

2.2. Preparation for Chitosan from Shrimp Shell Waste

Shrimp shell waste samples were obtained from one of the Micro, Small, and Medium Enterprises (UMKM) in Pasar Raya, Padang City. The wet shrimp shells were washed with tap water, dried under the solar light for 8 hours, then dried in an oven for 6 hours at 60°C. The dried shrimp shells were ground using a grinder, blended, and then sieved to 100 mesh. The powder was stored in a closed container before processing [11].

Chitosan extraction involves three steps: demineralization, deproteination, and deacetylation. In the demineralization stage, shrimp shells were treated with 1 M aqueous HCl in a 1:10 (w/v) ratio. This mixture was stirred at room temperature for 30 minutes and then allowed to stand for 12 hours. The demineralized sample was washed with deionized water until reaching a neutral pH and dried at 80°C for 24 hours. In the deproteination stage, the demineralized shrimp shells were mixed with a 4% (w/v) NaOH solution in a 1:20 (w/v) ratio and allowed to stand for 12 hours. The mixture was heated at 80°C and stirred using a hot plate for 4 hours.

The resulting product was washed with deionized water until reaching a neutral pH and then dried at 80°C for 24 hours to obtain chitin. Finally, in the stage, the chitin obtained was treated with 40% (w/v) concentrated NaOH solution in a 1:10 (w/v) ratio, heated to 90°C, and stirred on a hot plate for 2 hours. The product was washed with deionized water until reaching neutral pH and dried at 80°C for 24 hours. Then, the chitosan was stored for FTIR testing [1].

2.3. Synthesis of N-doped TiO_2 Nanoparticles

The synthesis of N-doped TiO_2 nanoparticles began by adding 1 mL of 1 M $TiCl_4$ solution dropwise into 10 mL of absolute ethanol, followed by adding 0.1 mL of concentrated HCl. The mixture was then transferred into a Teflon container and stirred with a magnetic stirrer for 30 minutes. Subsequently, 10% (w/w) chitosan was added, and the mixture was stirred for an additional hour. The resulting solution was placed in an autoclave and heated at 200°C for 16 hours. The obtained nanoparticles were washed with distilled water, dried at 80°C for 8 hours, and then calcined at 500°C for 1 hour. The final product was labeled as NTi10. The same procedure was repeated using different concentrations of chitosan—20% (w/w), 35% (w/w), and 50% (w/w)—to obtain NTi20, NTi35, and NTi50, respectively. A control sample, labeled TO, was synthesized using the same method without the addition of chitosan (i.e., undoped TiO_2) [12].

2.4. Photocatalytic Activity of N-doped TiO_2 Nanoparticles

The first step involved extracting microplastics from plastic bags. Ten grams of small pieces from crackle bags were added to 100 mL of boiling distilled water. After briefly cooling, the mixture was filtered using a sieve with a pore size of approximately 215 µm. The collected microplastics were then washed repeatedly with distilled water and dried at room temperature for 24 hours.

Photocatalytic experiments were conducted by adding 200 mg of microplastics into a glass container containing 50 mL of CH_3COONa/CH_3COOH buffer solution (0.4% w/v). Separately, 50 mL of 0.4% w/v polyethylene (PE) dispersion was added to 200 mg of the undoped TiO_2 photocatalyst labeled TO in a beaker. The mixture was stirred using an ultrasonicator for 15 minutes, then placed in a water bath at a distance of 25 cm from a 50-watt LED lamp at room temperature. The photocatalytic process was carried out for 50 hours with continuous stirring at 300 rpm.

The same procedure was repeated using TiO_2 samples prepared with different chitosan concentrations, labeled NTi10, NTi20, NTi35, and NTi50. The degradation performance of the microplastics was evaluated by measuring the percentage of mass loss (Equation 1) [13].

$$\text{Microplastic mass} = \frac{(M_0-M)}{M_0} \times 100\% \qquad (1)$$

Where, M_0 is the initial mass of microplastics before irradiation, and M is the microplastics after irradiation.

3. Results and Discussion

3.1. Vibrational Properties of Chitin and Chitosan

The results of FTIR characterization on chitin and chitosan compounds are shown in Figure 1. The FTIR spectrum of chitin exhibits a distinct absorption peak at a wavenumber of 3465 cm^{-1}, corresponding to the vibrational stretching of the hydroxyl (OH) group. Additionally, the wavenumbers at 3108 cm^{-1} and 1670 cm^{-1} are characteristic of amide II absorption, associated with the asymmetric bending of the —NH group, and amide I absorption, indicative of carbonyl (C=O) stretching vibrations, respectively. These features provide evidence of the presence of acetyl groups [14]. Then, the presence of chitosan is indicated by changes in the absorption peak around 3429 cm^{-1}, which becomes broader and shifts towards a smaller wave number; besides that, there is no peak on the Amide II absorption (asymmetric bending —NH). The appearance of a smaller Amide I absorption (C=O stretching vibration) in the FTIR spectrum of chitosan at 1621 cm^{-1} indicates the release of acetyl groups from chitin [15]. Based on the analysis of the above functional groups, it can be concluded that chitosan has been successfully obtained from shrimp shells.

3.2. Synthesized N-doped TiO_2 Nanoparticles

The synthesized N-doped TiO_2 nanoparticles are white powder for TO (without adding chitosan) and yellowish white for the NTi variation (chitosan addition), as shown in Figure 2. The yellowish white color for the NTi10, NTi20, NTi35, and NTi50 samples indicates that nitrogen doping has been successfully carried out [16].

3.3. Morphological Properties of Prepared N-doped TiO_2

FESEM characterization aims to study the surface morphology of the N-doped TiO_2 sample. The FESEM results of the N-doped TiO_2 (NTi50) sample with a magnification of 100,000 times are shown in Figure 3. The surface morphology of the sample is spherical. In addition, larger irregular grains with agglomeration are also observed, and the nanoparticles have a smooth surface. These findings suggest that the addition of chitosan as a nitrogen doping source does not significantly alter the morphological structure of TiO_2 [17]. Accurate measurement of the particle size is challenging due to clustering. Nevertheless, particle size plays a crucial role in determining the photocatalytic activity of the material, as smaller particles provide a higher surface area, offering more active sites for photocatalytic reactions [18].

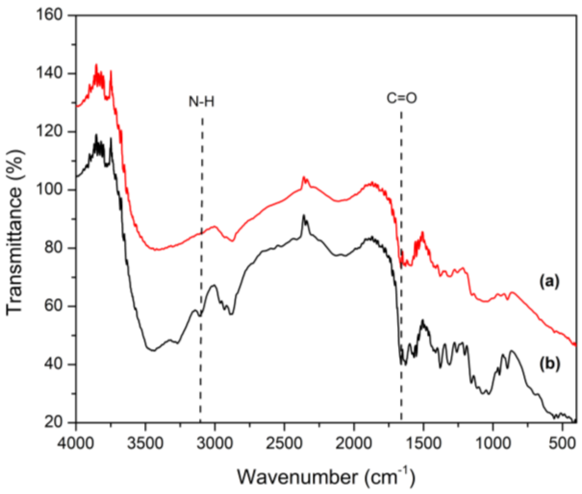

Figure 1. FTIR spectra of (a) chitin and (b) chitosan

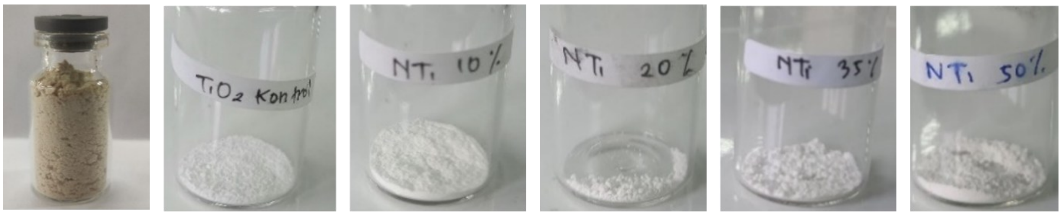

(a) (b) (c) (d) (e) (f)

Figure 2. Chitosan and all prepared nanoparticles: a) Chitosan, b) TO, c) NTi10, d) NTi20, e) NTi35, and f) NTi50

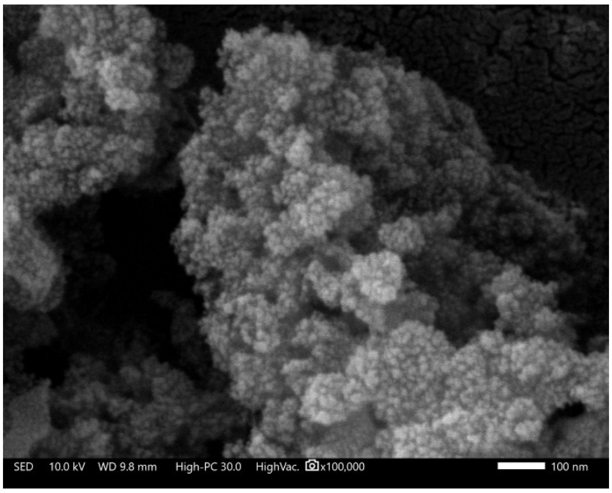

Figure 3. A typical FESEM image of NTi50 samples

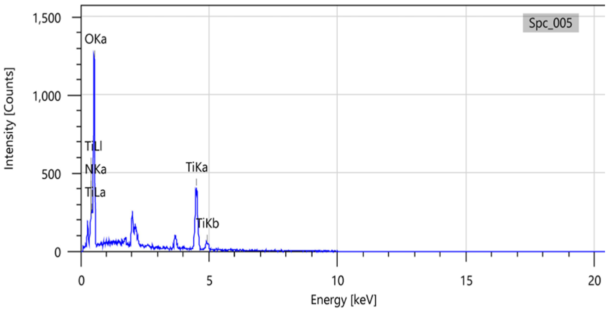

Figure 4. EDX spectra of the NTi50 sample

The elemental composition of the sample is illustrated using Energy Dispersive X-ray (EDX). The EDX spectrum in Figure 4 shows sharp peaks corresponding to titanium (Ti) and oxygen (O), which confirms the successful formation of titanium dioxide (TiO_2) as the primary phase. In addition, the presence of nitrogen (N) peaks in the spectrum indicates that nitrogen atoms have been successfully introduced into the TiO_2 lattice structure [19].

3.4. Structural Properties of Prepared N-doped TiO_2

XRD characterization was performed to determine the crystal phase, crystallite size, and crystallinity of the N-doped TiO_2 compounds. As presented in Figure 5, all N- doped TiO_2 samples exhibit diffraction patterns that are characteristic of the anatase phase of TiO_2, which aligns well with the ICSD (Inorganic Crystal Structure Database) standard number 44882 [2]. Notably, the main diffraction peak at $2\theta = 25.76°$, representing the dominant anatase plane, is shifted toward lower diffraction angles in the nitrogen-doped samples. This shift indicates the successful incorporation of nitrogen into the TiO_2 lattice structure [20]. The peak shift within the 2θ range of 20° to 28° is attributed to lattice expansion, which occurs due to the substitution of oxygen ions (O^{2-}, ionic radius $\approx$ 60 pm) with slightly larger nitrogen ions (N^{3-}, ionic radius $\approx$ 65 pm). This ionic substitution leads to an increase in interplanar spacing, as described by Bragg's law, thereby resulting in a shift of the diffraction peak to lower angles [10].

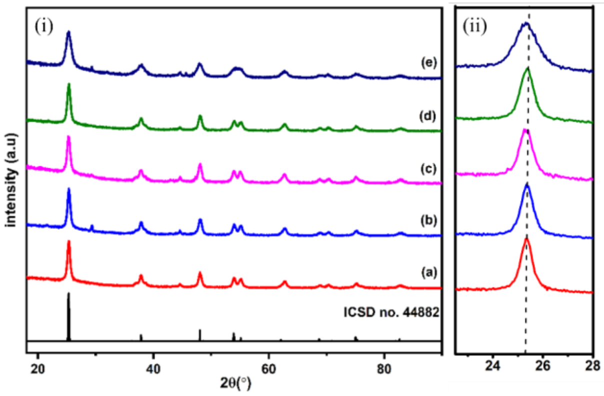

Figure 5. XRD patterns of : (i) (a) TO, (b) NTi10, (c) NTi20, (d) NTi35, (e) NTi50; (ii) magnified XRD patterns (Anatase 101 plane) of the N-doped TiO_2 samples between 20 and 28° (2θ)

The degree of crystallinity of N-doped TiO_2 nanoparticles was evaluated for various formulations: TO, NTi10, NTi20, NTi35, and NTi50, yielding values of 29.67%, 29.50%, 23.91%, 27.24%, and 30.61%, respectively. The size of the synthesized TiO_2 and N- doped TiO_2 crystals was determined using the Debye-Scherrer equation. The calculations revealed that the crystal size for TiO_2 nanoparticles, without incorporating chitosan, is 4.29 nm. In comparison, the crystal sizes of the N-doped TiO_2 nanoparticles—NTi10, NTi20, NTi35, and NTi50—were measured at 2.71 nm, 4.50 nm, 4.39 nm, and 1.95 nm, respectively. The observed reduction in crystal size following nitrogen doping can be attributed to the introduction of structural defects and lattice distortions, which are characteristic effects associated with nitrogen incorporation into the TiO_2 lattice [21].

3.5. Vibrational Properties of Prepared N-doped TiO_2 by Raman Spectroscopy Analysis

Raman spectroscopy is an important characterization tool that aims to study the properties of materials, such as phase transformation, crystallinity, and vibrational modes in N-doped TiO_2 samples. The Raman spectrum (Figure 6) shows peaks at 147, 197, 396, 514, and 636 cm^{-1} corresponding to $A_{1g}+2B_{1g}+3E_g$ modes, indicating the presence of the anatase phase. No additional peaks due to the nitrogen or rutile phase were seen [5]. The prominent peak appearing at 144 cm^{-1} is attributed to the extension vibration of the anatase structure.

In addition, it was observed that nitrogen-doped TiO_2 samples produced significant broadening and shifting of the Raman peak towards higher wave numbers, along with a decrease in intensity. This confirmed that nitrogen was successfully doped into the TiO_2 lattice. Moreover, these trends indicate that nitrogen doping disrupts the symmetry of TiO_2, leading to structural distortions. This disruption results in varying degrees of defects, namely oxygen vacancies, and inhibits the growth of TiO_2. All these factors result in differences in the frequencies of the vibrational modes, thus broadening and shifting the Raman peaks [6].

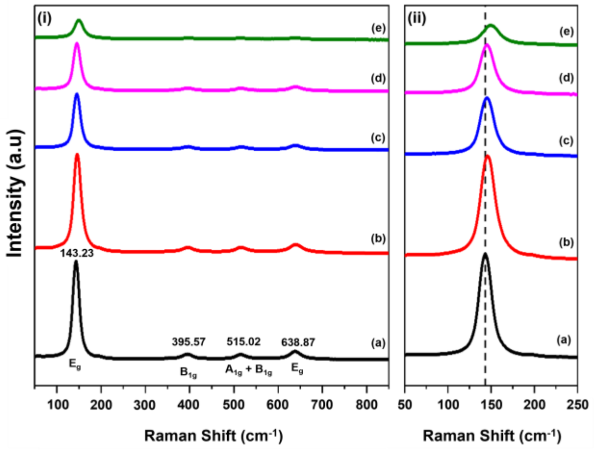

Figure 6. (i) Raman spectra of all samples: (a) TO, (b) NTi10, (c) NTi20, (d) NTi35, (e) NTi50, (ii) the enlarged Raman pattern of the N-doped TiO_2 sample between 50-280 cm^{-1}

3.6. Vibrational Properties of Prepared N-doped TiO_2 using FTIR Spectrophotometer

FTIR characterization aims to detect bond vibrations in the formation of N-doped TiO_2. Figure 7 shows that the vibrational absorption bands at wavenumbers 535-550 cm^{-1} are Ti—O—Ti stretch vibrations, indicating the formation of metal oxide bonds in the TiO_2 lattice [22]. The broad absorption peak at 3099-3334 cm^{-1} is caused by O—H stretch vibrations from H_2O absorbed on the surface of TiO_2. This O—H characteristic is beneficial in the photocatalytic process during the formation of hydroxyl radicals. Additionally, there is a small absorption peak at 1035 cm^{-1}, which is the N—Ti—O bond observed in NTi50, indicating that nitrogen from chitosan has been incorporated into TiO_2. However, in contrast to the other NTi variations, no absorption peak appears in the ~1000 cm^{-1} region due to the low chitosan concentration. The wavelength of ~1600 cm^{-1} is the bending vibration of the H—O—H bond caused by the physisorption of water molecules on the surface of TiO_2 [23].

3.7. Optical Properties of N-doped TiO_2

The characterization of N-doped TiO_2 nanoparticles using UV-Vis Diffuse Reflectance Spectroscopy (DRS) is designed to observe their light absorption properties and investigate their optical characteristics. Figure 8 shows that all N-doped TiO_2 nanoparticles absorb light within the visible region, at approximately 400 nm, indicating successful doping. The bandgap values of the samples were determined utilizing the Tauc Plot method.

As shown in Figure S1, the undoped TiO_2 sample exhibits an energy gap of 3.04 eV. Upon nitrogen doping, there is a noticeable reduction in the energy gap for the NTi10, NTi20, NTi35, and NTi50 samples, with values of 3.07 eV, 3.02 eV, 3.00 eV, and 2.97 eV, respectively [22]. This decrease in bandgap energy further confirms the successful incorporation of nitrogen into TiO_2. This phenomenon demonstrates that nitrogen dopants contribute to the narrowing of the photocatalyst's bandgap by forming a new N 2p band between the O 2p and Ti 3d orbitals within the valence band of the TiO_2 electronic structure [24].

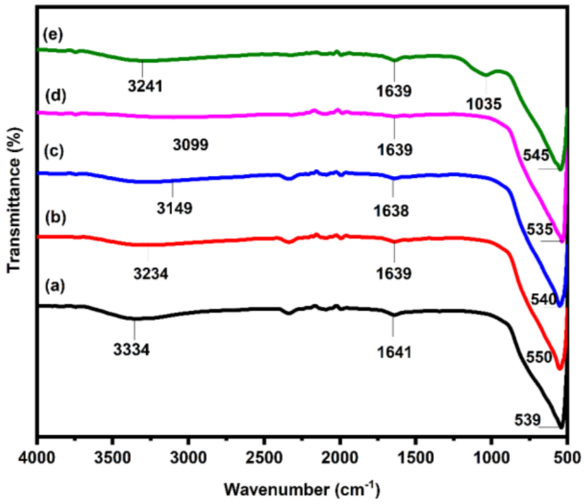

Figure 7. FTIR spectra of all samples: (a) TO, (b) NTi10, (c) NTi20, (d) NTi35, and (e) NTi50

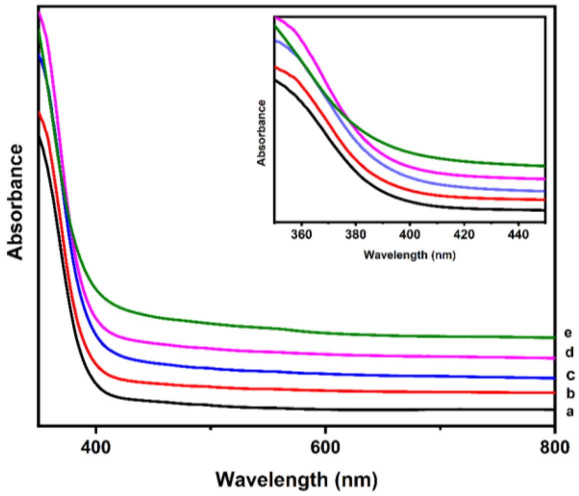

Figure 8. UV-Vis DRS spectra of: a) TO, b) NTi10, c) NTi20, d) NTi35, and e) NTi50

3.8. Photocatalytic Activity of N-doped TiO_2 Nanoparticles for Microplastics Degradation

The photocatalytic activity test evaluated the synthesized photocatalyst's effectiveness in degrading microplastics. The degradation test results, as shown in Figure 9 and Table 1, reveal that the N-doped TiO_2 sample with a nitrogen concentration of 50% by weight (NTi50) achieved the highest degradation percentage of 30.45% compared to other samples. This enhanced degradation is attributed to NTi50's superior optical properties and crystallinity. The results in the following experiments are related to the proposed reaction mechanism for the degradation of polyethylene microplastic [9].

$$TiO_2 \xrightarrow{hv} h^+{}_{VB} + e^-{}_{CB} \quad (2)$$

$$h^+{}_{VB} + H_2O \rightarrow {}^{\cdot}OH + H^+ \quad (3)$$

$${}^{\cdot}OH + \text{microplastic} \rightarrow CO_2 + H_2O \quad (4)$$

Based on Equations (2) to (4), OH radicals play an important role in degrading microplastics because OH radicals have a high reduction potential, allowing them to cleave chemical bonds in microplastic polymers in a non-selective manner, thus facilitating the conversion of these compounds into harmless end products [23].

Table 1. Photocatalytic performance of nitrogen-doped TiO_2 samples for the degradation of microplastics

Types of photocatalyst	% Degradation
TO (control)	5
NTi10	9.5
NTi20	17.86
NTi35	23.48
NTi50	30.45

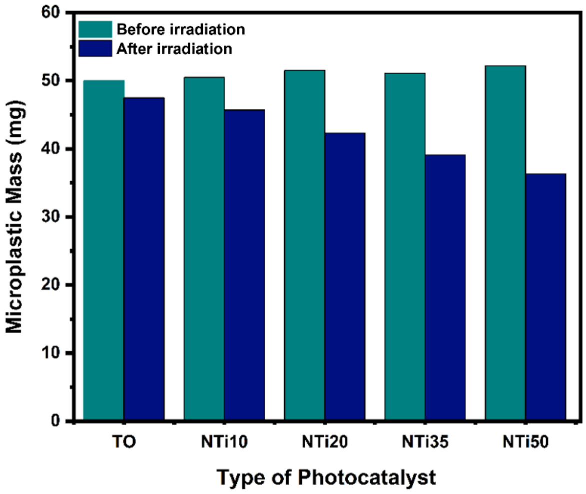

Figure 9. Photocatalytic activities of all samples

4. Conclusion

In conclusion, chitosan derived from waste shrimp shells emerges as a promising nitrogen source for doping TiO_2, enhancing its properties and ability to degrade microplastics. Although nitrogen from an organic origin did not significantly alter the crystalline structure of TiO_2, it substantially improved the material's capacity to absorb visible light and reduced its bandgap. Furthermore, nitrogen obtained from chitosan substantially enhanced the photocatalytic performance of TiO_2 in degrading polyethylene microplastics. Specifically, the 50% nitrogen-doped TiO_2 exhibited a degradation rate of 30.45% in an aqueous solution under 50 hours of visible light irradiation, which is six times greater than that of pristine white TiO_2. This demonstrates the effectiveness of using chitosan as a doping agent to enhance the performance of TiO_2 in environmental applications.

Acknowledgments

The authors express their sincere gratitude to the Indonesian Directorate General of Learning and Student Affairs, Ministry of Education, Culture, Research and Technology, and Andalas University, through the Student Creativity Program 2024 [001734722205000].

References

[1] Rawintra Eamrat, Suphatchai Rujakom, Tatchai Pussayanavin, Achara Taweesan, Chayanid Witthayaphirom, Tatsuru Kamei, Optimizing biocoagulant aid from shrimp shells (*Litopenaeus vannamei*) for enhancing microplastics removal from aqueous solutions, *Environmental Technology & Innovation*, 33, (2024), 103457 https://doi.org/10.1016/j.eti.2023.103457

[2] Surya Singh, Tanwi Trushna, Madhanraj Kalyanasundaram, Ashok J. Tamhankar, Vishal Diwan, Microplastics in drinking water: a macro issue, *Water Supply*, 22, 5, (2022), 5650-5674 https://doi.org/10.2166/ws.2022.189

[3] Sherri A. Mason, Victoria G. Welch, Joseph Neratko, Synthetic Polymer Contamination in Bottled Water, *Frontiers in Chemistry*, 6, (2018), https://doi.org/10.3389/fchem.2018.00407

[4] Elinda Eka Putri, Indang Dewata, Optimasi Konsentrasi Hidrogen Peroksida (H_2O_2) Metode Wet Peroxide Oxidation untuk Identifikasi Mikroplastik Polyethylene Terephthalate (PET), *Jurnal Pendidikan Tambusai*, 7, 3, (2023), 24736-24743

[5] Didit Ardi Maulana, Muhammad Ibadurrohman, Slamet, Synthesis of Nano-Composite Ag/TiO_2 for Polyethylene Microplastic Degradation Applications, *IOP Conference Series: Materials Science and Engineering*, 1011, 1, (2021), 012054 https://doi.org/10.1088/1757-899X/1011/1/012054

[6] Yanling He, Atta Ur Rehman, Muxian Xu, Christelle A. Not, Alan M. C. Ng, Aleksandra B. Djurišić, Photocatalytic degradation of different types of microplastics by TiO_x/ZnO tetrapod photocatalysts, *Heliyon*, 9, 11, (2023), e22562 https://doi.org/10.1016/j.heliyon.2023.e22562

[7] Abdusalam Uheida, Hugo Giraldo Mejía, Mohamed Abdel-Rehim, Wael Hamd, Joydeep Dutta, Visible light photocatalytic degradation of polypropylene microplastics in a continuous water flow system, *Journal of Hazardous Materials*, 406, (2021), 124299 https://doi.org/10.1016/j.jhazmat.2020.124299

[8] Xiaoyou Yu, Qianrui Lv, N doping of TiO_2 nanocrystal for efficient photodegradation of organic pollutants underultraviolet and visible light irradiation, *Turkish Journal of Chemistry*, 45, 5, (2021), 1366-1374 https://doi.org/10.3906/kim-2103-7

[9] Maria Camila Ariza-Tarazona, Cristina Siligardi, Hugo Alejandro Carreón-López, José Enrique Valdéz-Cerda, Paolo Pozzi, Garima Kaushik, Juan Francisco Villarreal-Chiu, Erika Iveth Cedillo-González, Low environmental impact remediation of microplastics: Visible-light photocatalytic degradation of PET microplastics using bio-inspired C,N-TiO_2/SiO_2 photocatalysts, *Marine Pollution Bulletin*, 193, (2023), 115206 https://doi.org/10.1016/j.marpolbul.2023.115206

[10] Lei Dai, Peng Fu, Jieming Chen, Fazhe Sun, Nitrogen doping mediated oxygen vacancy and Ti valence regulation to enhance photocatalytic H_2 generation, *International Journal of Hydrogen Energy*, 48, 67, (2023), 26187-26199 https://doi.org/10.1016/j.ijhydene.2023.03.344

[11] Istianah Nur Isnaeni, Indriyati, Dedi, Dadan Sumiarsa, Indah Primadona, Green synthesis of different TiO_2 nanoparticle phases using mango-peel extract, *Materials Letters*, 294, (2021), 129792 https://doi.org/10.1016/j.matlet.2021.129792

[12] Erlandy Dwinanto Toe, Winarto Kurniawan, Eden G. Mariquit, Hirofumi Hinode, Synthesis of N-doped mesoporous TiO_2 by facile one-step solvothermal process for visible light photocatalytic degradation

of organic pollutant, *Journal of Environmental Chemical Engineering*, 6, 4, (2018), 5125-5134 https://doi.org/10.1016/j.jece.2018.08.005

[13] Yin-Cheng Yen, Sheng Ou, Kuan-Jiuh Lin, One-Pot Synthesis of Nitrogen-doped TiO_2 Nanowires with Enhanced Photocurrent Generation, *Journal of the Chinese Chemical Society*, 64, 12, (2017), 1392-1398 https://doi.org/10.1002/jccs.201700226

[14] Prisma Trida Hardani, Dewi Perwito, Nadia Aisah Mayzika, Review Artikel: Isolasi Kitin Dan Kitosan Dari Berbagai Sumber Bahan Alam, *Seminar Nasional Hasil Riset dan Pengabdian*, 3, (2021), 469-475

[15] Majid Pakizeh, Ali Moradi, Toktam Ghassemi, Chemical extraction and modification of chitin and chitosan from shrimp shells, *European Polymer Journal*, 159, (2021), 110709 https://doi.org/10.1016/j.eurpolymj.2021.110709

[16] Maria Camila Ariza-Tarazona, Juan Francisco Villarreal-Chiu, Juan Manuel Hernández-López, Javier Rivera De la Rosa, Virginia Barbieri, Cristina Siligardi, Erika Iveth Cedillo-González, Microplastic pollution reduction by a carbon and nitrogen-doped TiO_2: Effect of pH and temperature in the photocatalytic degradation process, *Journal of Hazardous Materials*, 395, (2020), 122632 https://doi.org/10.1016/j.jhazmat.2020.122632

[17] Pratibha V. Bakre, S. G. Tilve, R. N. Shirsat, Influence of N sources on the photocatalytic activity of N-doped TiO_2, *Arabian Journal of Chemistry*, 13, 11, (2020), 7637-7651 https://doi.org/10.1016/j.arabjc.2020.09.001

[18] I. Putu Mahendra, Adri Huda, Ha Minh Ngoc, Phan Trung Nghia, Tamrin Tamrin, Basuki Wirjosentono, Investigation of TiO_2 doped with nitrogen and vanadium using hydrothermal/Sol-Gel method and its application for dyes photodegradation, *Arab Journal of Basic and Applied Sciences*, 26, 1, (2019), 242-253 https://doi.org/10.1080/25765299.2019.1610209

[19] Diana Vanda Wellia, Atika Syafawi, Yulia Eka Putri, Muldarisnur, The effect of cetyltrimethylammonium bromide (CTAB) addition on green synthesis of porous N-doped TiO_2 for photoreduction of heavy metal ion Cr(VI), *RSC Advances*, 13, 42, (2023), 29645-29656 https://doi.org/10.1039/d3ra03247g

[20] Nufus Kanani, Teguh Kurniawan, Widya Kosimaningrum, Yenny Meliana, Jayanudin, Endarto Wardhono, Ultrasonic irradiation as a mild and efficient protocol for the demineralization of chitin from shrimp shell wastes, *South African Journal of Chemical Engineering*, 43, (2023), 359-368 https://doi.org/10.1016/j.sajce.2022.12.004

[21] Chaehun Lim, Ha-Rim An, Seongmin Ha, Seongjae Myeong, Chung Gi Min, Hea-Jong Chung, Byoungchul Son, Chang-Yeon Kim, Ji-In Park, Hyeran Kim, Hyun Uk Lee, Young-Seak Lee, Highly visible-light-responsive nanoporous nitrogen-doped TiO_2 (N-TiO_2) photocatalysts produced by underwater plasma technology for environmental and biomedical applications, *Applied Surface Science*, 638, (2023), 158123 https://doi.org/10.1016/j.apsusc.2023.158123

[22] Javed Ali Khan, Murtaza Sayed, Noor S. Shah, Sanaullah Khan, Ashfaq Ahmad Khan, Muhammad Sultan, Ammar M. Tighezza, Jibran Iqbal, Grzegorz Boczkaj, Synthesis of N-doped TiO_2 nanoparticles with enhanced photocatalytic activity for 2,4-dichlorophenol degradation and H_2 production, *Journal of Environmental Chemical Engineering*, 11, 6, (2023), 111308 https://doi.org/10.1016/j.jece.2023.111308

[23] Brenda Estefanía Llorente-García, Juan Manuel Hernández-López, Antonio Alberto Zaldívar-Cadena, Cristina Siligardi, Erika Iveth Cedillo-González, First Insights into Photocatalytic Degradation of HDPE and LDPE Microplastics by a Mesoporous N–TiO2 Coating: Effect of Size and Shape of Microplastics, *Coatings*, 10, 7, (2020), 658 https://doi.org/10.3390/coatings10070658

[24] Nacer Boudouaia, Zohra Bengharez, Salah Jellali, Preparation and characterization of chitosan extracted from shrimp shells waste and chitosan film: application for Eriochrome black T removal from aqueous solutions, *Applied Water Science*, 9, 4, (2019), 91 https://doi.org/10.1007/s13201-019-0967-z